

RESEARCH

Open Access

# Enhanced luminescence intensity of novel red-emitting phosphor - $\text{Sr}_3\text{Lu}_2(\text{BO}_3)_4:\text{Bi}^{3+}, \text{Eu}^{3+}$ via energy transfer

Irish Valerie B Maggay, Pin-Chun Lin and Wei-Ren Liu\*

\* Correspondence:  
WRLiu1203@gmail.com  
Department of Chemical  
Engineering, Chung Yuan Christian  
University, 200 Chung Pei Rd.,  
Chung Li City 32023, Taiwan

## Abstract

$\text{Bi}^{3+}/\text{Eu}^{3+}$  co-activated  $\text{Sr}_3\text{Lu}_2(\text{BO}_3)_4$  was successfully synthesized via a solid state reaction. The optimal concentration of  $\text{Bi}^{3+}$ ,  $\text{Eu}^{3+}$  and  $\text{Bi}^{3+}/\text{Eu}^{3+}$  are 1 mol%, 60 mol% and 1 mol%/20 mol%, respectively. The emission spectra of  $\text{Sr}_3\text{Lu}_2(\text{BO}_3)_4:\text{Bi}^{3+}, \text{Eu}^{3+}$  gives three peaks located at 405 nm, 489 nm which were attributed to  $\text{Bi}^{3+}$   $S_6$  (blue) and  $C_2$  (green) site symmetry, respectively and 610 nm which was ascribed to  $\text{Eu}^{3+}$  ( $^5\text{D}_0 \rightarrow ^7\text{F}_2$ ) transition. The emission intensity of  $\text{Bi}^{3+}$  decreases with increasing  $\text{Eu}^{3+}$  content which indicates that a efficient energy transfer occurred in the  $\text{Sr}_3\text{Lu}_2(\text{BO}_3)_4$  host. The relative intensity of  $\text{Sr}_3\text{Lu}_{1.79}(\text{BO}_3)_4:0.01\text{Bi}^{3+}, 0.20\text{Eu}^{3+}$  excited at 327 nm and 370 nm was remarkably enhanced by 201% and 265%, respectively, via the energy transfer from  $\text{Bi}^{3+}$  to  $\text{Eu}^{3+}$ . The results indicate that  $\text{Sr}_3\text{Lu}_2(\text{BO}_3)_4:\text{Bi}^{3+}, \text{Eu}^{3+}$  is a potential novel red-emitting phosphor for UV LED applications.

**Keywords:**  $\text{Bi}^{3+}/\text{Eu}^{3+}$  co-doping; Red-emitting phosphor; Solid state reaction

## Background

Recently, there has been a rapid increase in the number of researches on white-light emitting diodes (W-LEDs) and it has begun replacing conventional lighting sources due to its advantages such as high brightness, high energy efficiency, low power consumption, longer working performance and low environmental risk [1-6]. The common fabrication of W-LEDs involves a blue-emitting InGaN chip and a yellow emitting phosphor  $\text{Y}_3\text{Al}_5\text{O}_{12}:\text{Ce}^{3+}$  (YAG) [1,2,7]. However, this combination displays low color rendering index ( $R_a$ ) of ~80 and high color temperature which is due to the insufficiency of red emission in the visible spectrum [5]. Thus, it is very essential to search for new red phosphors that can be efficiently excited at around 400 nm [8].

$\text{Eu}^{3+}$  rare earth ions have drawn much attention of scientists in obtaining a red-emitting due to its lowest excited level  $^5\text{D}_0$  of the  $4f^6$  configuration which is located below the  $4f^65d$  configuration and it principally displays very sharp red emission lines at  $^5\text{D}_0 \rightarrow ^7\text{F}_2$  transition around 610 ~ 618 nm [8,9]. Most of the red-emitting phosphors are efficiently excited at around 393 nm [10,11] originating from  $^7\text{F}_0 \rightarrow ^5\text{L}_6$  transition which is parity forbidden therefore it exists as a sharp peak and cannot absorb the excitation energy efficiently. In order to improve and broaden the excitation spectrum of  $\text{Eu}^{3+}$  ions, one of the common strategies is by introducing  $\text{Bi}^{3+}$  as a sensitizer. Liu et al. [1] found that the luminescence intensity and quantum efficiency of  $\text{ZnB}_2\text{O}_4:\text{Bi}^{3+}, \text{Eu}^{3+}$

phosphors were much higher than that of  $\text{ZnB}_2\text{O}_4\cdot\text{Eu}^{3+}$  phosphors by co-doping  $\text{Bi}^{3+}$  into the host via an energy transfer process. The optimized-composition of  $\text{ZnB}_2\text{O}_4\cdot\text{Eu}^{3+}$ ,  $\text{Bi}^{3+}$  was even superior to that of commercial phosphor,  $\text{La}_2\text{O}_2\text{S}\cdot\text{Eu}^{3+}$ . Zhou et al. [4] reported that the enhanced luminescence properties and energy transfer mechanism of  $\text{Ca}_3\text{Sn-Si}_2\text{O}_9\cdot\text{Bi}^{3+}$ ,  $\text{Eu}^{3+}$  phosphors by a solid state reaction. Zhu et al. [9] investigated the energy transfer phenomena of  $\text{Bi}^{3+}/\text{Eu}^{3+}$  co-doped  $\text{Ca}_{10}(\text{PO}_4)_6\text{F}_2$  phosphors for UVLED applications. Park et al. [12] discovered that with increasing the content of  $\text{Bi}^{3+}$  on  $\text{Eu}^{3+}/\text{Bi}^{3+}$  co-doping  $\text{YVO}_4\cdot\text{Eu}^{3+}$  phosphors, it demonstrate a shifting of the excitation band to a longer wavelength due to the energy transfer from  $\text{Bi}^{3+}$  to  $\text{Eu}^{3+}$ . Single-phased phosphors have attracted much attention in the fabrication of white LED and borate compounds are good candidates because they can be easily synthesized and are chemically stable. To the best of our knowledge, spectral and laser properties of  $\text{Er:Yb Sr}_3\text{Lu}_2(\text{BO}_3)_4$  have been reported and it have manifested good spectral properties. Moreover, a study was carried on the luminescent characteristics of  $\text{Sr}_3(\text{RE})_2(\text{BO}_3)_4\cdot\text{Dy}^{3+}$  ( $\text{RE} = \text{Y, La, Gd}$ ) for white LED applications and provided a significant evidence.

To the best of our knowledge, there has been no reported study on the luminescence properties of  $\text{Bi}^{3+}/\text{Eu}^{3+}$  co-doped  $\text{Sr}_3\text{Lu}_2(\text{BO}_3)_4$ . In this study, crystal structure, phase purities as well as luminescence and energy transfer mechanism of  $\text{Sr}_3\text{Lu}_2(\text{BO}_3)_4\cdot\text{Bi}^{3+}$ ,  $\text{Eu}^{3+}$  phosphors were firstly investigated. The results demonstrate that  $\text{Sr}_3\text{Lu}_2(\text{BO}_3)_4\cdot\text{Bi}^{3+}$ ,  $\text{Eu}^{3+}$  is a potential red-emitting phosphor for UVLED applications.

## Methods

Polycrystalline powder samples were prepared via a solid state reaction. The starting materials used were  $\text{SrCO}_3$  (99.99%, Aldrich),  $\text{H}_3\text{BO}_3$  (99.99%, Strem),  $\text{Lu}_2\text{O}_3$  (99.99% Aldrich),  $\text{Eu}_2\text{O}_3$  (99.99%, Aldrich) and  $\text{Bi}_2\text{O}_3$  (99.99%Aldrich) were weighed in stoichiometric ratios and were homogeneously mixed and ground in agate mortar then transferred in alumina crucibles and sintered at  $1200^\circ\text{C}$  for 8 hours in air. The products were cooled down to ambient temperature and pulverized for further analysis.

The phase purity of the as-synthesized samples were characterized using X-ray diffraction (XRD) patterns with  $\text{Cu K}\alpha$  radiation ( $\lambda = 0.15418 \text{ \AA}$ ) generated at 45 kV and 30 mA. Data were collected in the  $2\theta$  range of  $10\text{--}80^\circ$  with a scan speed of  $5^\circ/\text{min}$ . The PL/PLE spectra of  $\text{Bi}^{3+}/\text{Eu}^{3+}$  co-doped  $\text{Sr}_3\text{Lu}_2(\text{BO}_3)_4$  phosphors were measured at room temperature and recorded by a Spex Fluorolog-3 spectrophotometer equipped with 450 W Xenon light source. All the spectra were measured with a scan rate of  $150 \text{ nm min}^{-1}$ . The Commission International de l'Eclairage (CIE) chromaticity coordinates were measured by a Laiko DT-101 color analyzer equipped with a CCD detector (Laiko Co., Tokyo, Japan).

## Results and discussion

### XRD and crystal structure analyses

The XRD patterns of  $\text{Sr}_3\text{Lu}_2(\text{BO}_3)_4$  doped with (a) 1 mol%  $\text{Bi}^{3+}$ , (b) 60 mol%  $\text{Eu}^{3+}$  and (c) 1 mol%  $\text{Bi}^{3+}/20 \text{ mol\% Eu}^{3+}$  and (d) standard pattern of ICSD 10213 are shown in Figure 1. The results show that the as-synthesized  $\text{Sr}_3\text{Lu}_2(\text{BO}_3)_4$  and  $\text{Bi}^{3+}$ ,  $\text{Eu}^{3+}$  or  $\text{Bi}^{3+}/\text{Eu}^{3+}$  co-doped  $\text{Sr}_3\text{Lu}_2(\text{BO}_3)_4$  are in well consistent with standard pattern of ICSD 10213, indicating that single-phased phosphors were successfully obtained by a solid state reaction. In addition, there are no notable peak shifts while doping  $\text{Bi}^{3+}$  and  $\text{Eu}^{3+}$  ions into the host,

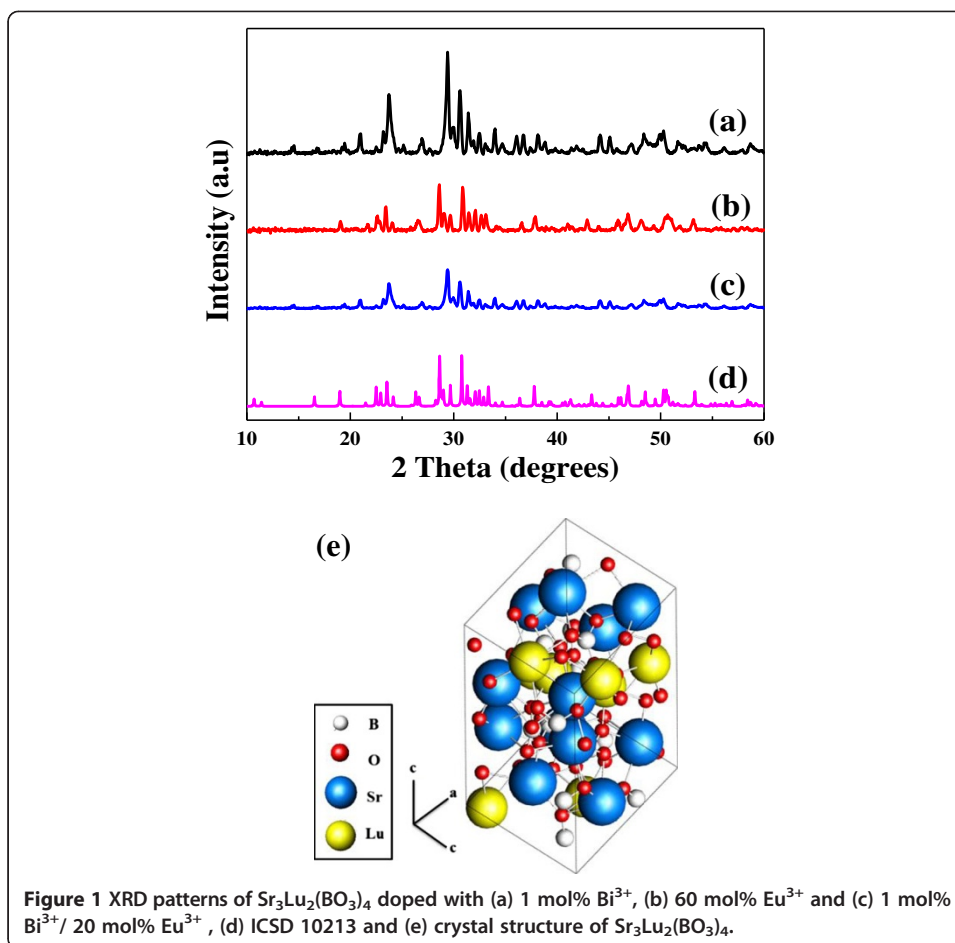


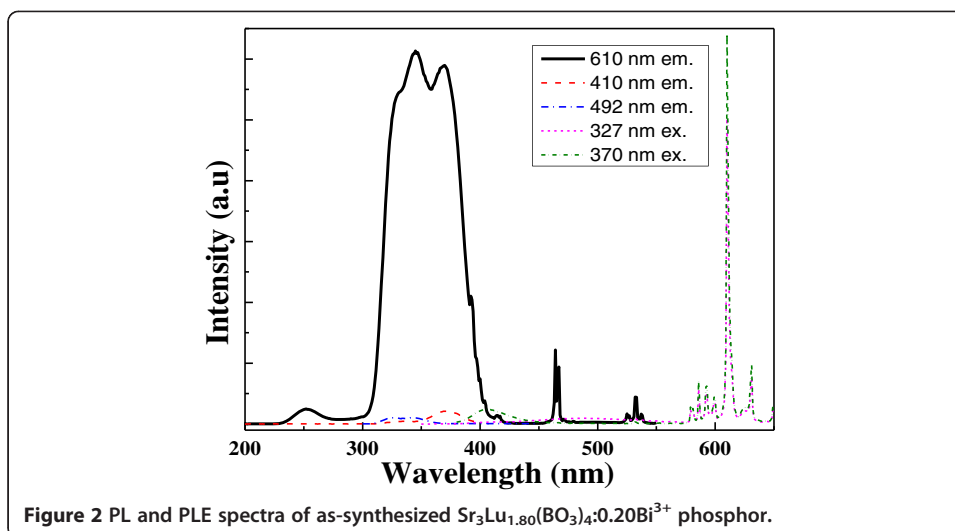
**Figure 1** XRD patterns of  $\text{Sr}_3\text{Lu}_2(\text{BO}_3)_4$  doped with (a) 1 mol%  $\text{Bi}^{3+}$ , (b) 60 mol%  $\text{Eu}^{3+}$  and (c) 1 mol%  $\text{Bi}^{3+}$ / 20 mol%  $\text{Eu}^{3+}$ , (d) ICSD 10213 and (e) crystal structure of  $\text{Sr}_3\text{Lu}_2(\text{BO}_3)_4$ .

which demonstrates that  $\text{Bi}^{3+}$  and  $\text{Eu}^{3+}$  ions are completely dissolved in the host lattice as a solid solution by occupying the  $\text{Lu}^{3+}$  sites due to their similar ionic radii of 0.977 Å, 1.11 Å and 1.07 Å for  $\text{Lu}^{3+}$ ,  $\text{Bi}^{3+}$  and  $\text{Eu}^{3+}$ , respectively [4,13]. The host phosphor belongs to  $\text{Sr}_3\text{RE}_2(\text{BO}_3)_4$  (RE:  $\text{Gd}^{3+}$ ,  $\text{Y}^{3+}$ ,  $\text{La}^{3+}$  and  $\text{Lu}^{3+}$ ) system which has an orthorhombic structure with  $\text{Pc}21n$  space group. The lattice parameters of  $\text{Sr}_3\text{Y}_2(\text{BO}_3)_4$  has lattice parameters of  $a = 8.701(1)$  Å,  $b = 15.984(8)$  Å,  $c = 7.381(2)$  Å and  $\alpha = \beta = \gamma = 90^\circ$  [14,15]. Furthermore, the longer distance among the rare-earth ions in the crystal structure of  $\text{Sr}_3\text{Y}_2(\text{BO}_3)_4$  results in higher doping concentration of  $\text{Eu}^{3+}$  [14].

Figure 1(e) displays the crystallographic structure. The  $\text{Sr}_3\text{Lu}_2(\text{BO}_3)_4$   $\text{Lu}^{3+}$  ions occupy two distinct crystallographic sites  $\text{Lu}_1$  and  $\text{Lu}_2$  and each  $\text{Lu}^{3+}$  has an eight-fold coordination that forms  $\text{LuO}_8$  polyhedra. The bond valence of  $\text{Lu}_1$  is stronger compared to  $\text{Lu}_2$ , therefore  $\text{Bi}^{3+}$  and  $\text{Eu}^{3+}$  occupies the  $\text{Lu}^{3+}$  site. Figure 1. XRD patterns of  $\text{Sr}_3\text{Lu}_2(\text{BO}_3)_4$  doped with (a) 1 mol%  $\text{Bi}^{3+}$ , (b) 60 mol%  $\text{Eu}^{3+}$ , (c) 1 mol%  $\text{Bi}^{3+}$ , 20 mol%  $\text{Eu}^{3+}$ , (d) ICSD 10213 and (e) crystal structure of  $\text{Sr}_3\text{Lu}_2(\text{BO}_3)_4$ .

#### Photoluminescence properties of $\text{Sr}_3\text{Lu}_2(\text{BO}_3)_4:\text{Bi}^{3+}$ phosphors

The PL and PLE of spectra of  $\text{Sr}_3\text{Lu}_{1.8}(\text{BO}_3)_4:0.20\text{Bi}^{3+}$  phosphor are illustrated in Figure 2. When the samples are excited at 327 nm and 335 nm, the emission spectra displays three broad bands centering at 356 nm, 405 nm emitting blue color and 485 nm emitting green color however if the phosphors are excited at 370 nm, the emission spectra contains one

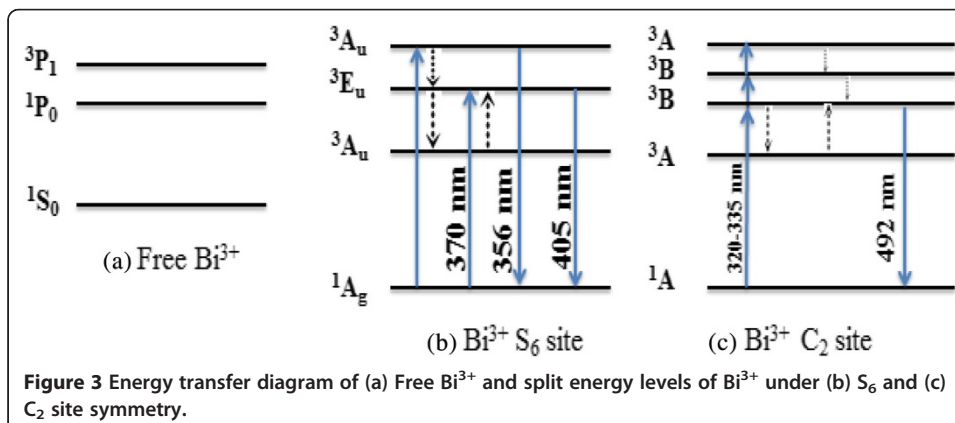


broad band with peak maximum at 404 nm. Varying the excitation wavelengths from 320 ~ 370 nm greatly affects the emission spectra of  $\text{Sr}_3\text{Lu}_2(\text{BO}_3)_4:\text{x}\%\text{Bi}^{3+}$ . Therefore, the energy distribution of blue and green emission is highly dependent on the excitation wavelengths.

The excitation spectrum monitored at 492 nm (green emission) consists of two peaks at 326 nm and 342 nm respectively meanwhile the excitation spectrum monitored at 410 nm (blue emission) consists of a weak broad band at 334 nm and a strong broad band at 371 nm. If the  $\text{Bi}^{3+}$  ion is asymmetrically coordinated, the Stokes shift of  $\text{Bi}^{3+}$  is large. Therefore, the blue emission and green emission originates from  $S_6$  and  $C_2$  symmetry respectively [15].

Figure 3 shows the energy level diagram of  $\text{Bi}^{3+}$  under  $S_6$  and  $C_2$  symmetry. The emission band with maximum peaks at 356 nm and 405 nm are attributed to  ${}^3A_u \rightarrow {}^1A_g$  and  ${}^3E_u \rightarrow {}^1A_g$  of  $S_6$  respectively. On the other hand, the excitation peaks at 335 nm and 370 nm found at site  $S_6$  are ascribed to  ${}^1A_g \rightarrow {}^3A_u$ . The green emission band with maximum peak at 485 nm is due to  ${}^3B \rightarrow {}^1A$  transition while the excitation peaks at 327 nm and 335 nm responsible for the green emission due to  ${}^1A \rightarrow {}^3B$  transition under  $C_2$  site symmetry of  $\text{Bi}^{3+}$  [15].

The  $\text{Sr}_3\text{Lu}_2(\text{BO}_3)_4:\text{Bi}^{3+}$  phosphors display efficient luminescence properties at ambient temperature. The luminesce properties of various concentrations of  $\text{Bi}^{3+}$  in the



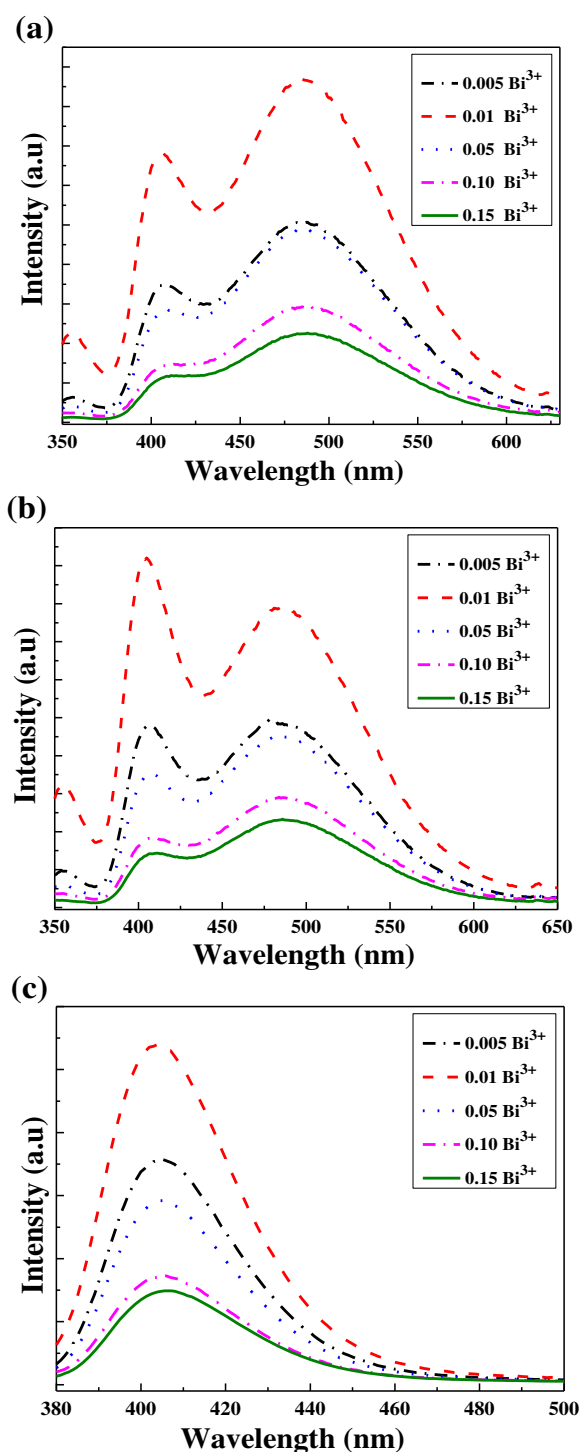
range of 0.005-0.15. in  $\text{Sr}_3\text{Lu}_2(\text{BO}_3)_4$  host are shown in Figure 4. It was noticeable that the emission intensity increased with the increasing amount of  $\text{Bi}^{3+}$  concentration until 1 mol%, and began to decrease due to concentration quenching. Generally, concentration quenching of luminescence was attributable to the energy migration existing among the activator ions at high concentration. During this migration process, the excitation energy would be diminished at a quenching site, causing a decrease in the luminescence [3]. Thus, the optimum concentration of  $\text{Bi}^{3+}$  in  $\text{Sr}_3\text{Lu}_2(\text{BO}_3)_4:\text{Bi}^{3+}$  was determined to be 0.01. It was also notable in the emission bands that the luminescent centers of  $\text{Bi}^{3+}$  at  $S_6$  and  $C_2$  quench simultaneously although they have different Stokes shift and concentration.  $C_2$  has higher concentration of  $\text{Bi}^{3+}$  than that of  $S_6$  which is essential for concentration quenching. However, higher Stokes shift leads to lower spectral overlap, offsetting the concentration quenching effect. Ju et al. [15] proposed that the energy transfer from  $\text{Bi}^{3+}$  under  $C_2$  site to  $\text{Bi}^{3+}$  under  $S_6$  site may be the reason to this phenomenon. As shown in Figure 3, the emission band of  $\text{Bi}^{3+}$  under  $C_2$  overlaps the excitation band of  $\text{Bi}^{3+}$  under  $S_6$ . Conversely, if the emission band of  $\text{Bi}^{3+}$  under  $C_2$  does not overlap the excitation band of  $\text{Bi}^{3+}$  under  $S_6$  it cannot overlap its own excitation band which is situated at much higher energy. Moreover, the excitation spectra of  $\text{Bi}^{3+}$  at  $C_2$  coincides with the excitation spectra of  $\text{Bi}^{3+}$  at  $S_6$  from 300 nm – 350 nm although they have different absorption profiles but nonetheless, this is an obvious evident for  $\text{Bi}^{3+}$ - $\text{Eu}^{3+}$  energy transfer.

Figure 5 shows the normalized intensity of  $\text{Sr}_3\text{Lu}_2(\text{BO}_3)_4:\text{Bi}^{3+}$  phosphors excited at 327 nm, 335 nm and 370 nm. The emission intensity of the phosphors gradually increased with the increasing amount of  $\text{Bi}^{3+}$  until 0.01 mole and started to decrease when the concentration of  $\text{Bi}^{3+}$  was further increased. Also, the emission intensity with respect to  $\text{Bi}^{3+}$  concentration was consistent among the three excitation wavelengths.

#### Photoluminescence properties of $\text{Sr}_3\text{Lu}_2(\text{BO}_3)_4:\text{Eu}^{3+}$ phosphors

The photoluminescence of  $\text{Sr}_3\text{Lu}_2(\text{BO}_3)_4:\text{Eu}^{3+}$  phosphors are displayed in Figures 6. The emission spectra excited at 393 nm displays sharp peaks at 578 nm, 591 nm, 610 nm, 650 nm and 700 nm which were attributed to the  $^5\text{D}_0 \rightarrow ^7\text{F}_j$  ( $j = 0,1,2,3,4$ ) transitions of  $\text{Eu}^{3+}$  ions respectively. The highest peak which was situated at 610 nm produced a red-emitting phosphor. Due to the absence of inversion symmetry and the break of parity selection rules,  $^5\text{D}_0 \rightarrow ^7\text{F}_2$  electric dipole is the strongest transition [4]. The excitation spectrum of  $\text{Sr}_3\text{Lu}_2(\text{BO}_3)_4:\text{Eu}^{3+}$  is also scrutinized. The broad band at 230 nm – 280 nm was due to the charge transfer band transition coming from ion  $\text{O}_2^-$  to  $\text{Eu}^{3+}$ . The narrow bands and sharp peaks found at 300 nm – 500 nm were ascribed to the intra-configurational  $4f$ - $4f$  transitions of  $\text{Eu}^{3+}$ .

Figure 7a shows the emission spectra of  $\text{Sr}_3\text{Lu}_{2-y}(\text{BO}_3)_4:y\text{Eu}^{3+}$  phosphors with  $x = 0.20, 0.40, 0.60$  and  $0.80$  under 393 nm excitation. The emission spectra are dominated by a large peak located at 610 nm ascribed to the  $^5\text{D}_0 \rightarrow ^7\text{F}_2$  transition this indicates that the  $\text{Eu}^{3+}$  ions occupy non-inversion symmetry sites which is in accordance to the point group  $C_1$ . Figure 7b shows the relationship of the luminescence intensity at 610 nm as a function of its doping concentration ( $x$ ) excited at 393 nm. Initially, the emission intensity increases as the doping concentration of  $\text{Eu}^{3+}$  increases due to the increase of absorption centers and reaches a maximum of 60 mol% and eventually drops with further increase in the concentration due to concentration quenching.



**Figure 4** Emission spectra of as-synthesized  $\text{Sr}_3\text{Lu}_2(\text{BO}_3)_4:\text{xBi}^{3+}$  phosphor excited at (a) 327 nm, (b) 335 nm and (c) 370 nm.

#### Photoluminescence properties of $\text{Sr}_3\text{Lu}_{1.99-\text{y}}(\text{BO}_3)_4:0.01\text{Bi}^{3+}, \text{yEu}^{3+}$ phosphors

The emission and excitation spectra of  $\text{Sr}_3\text{Lu}_{1.79}(\text{BO}_3)_4:0.01\text{Bi}^{3+}, 0.20\text{Eu}^{3+}$  phosphors are depicted in Figure 8. The emission spectra were investigated and analyzed by exciting the sample at 327 nm and 370 nm. The emission spectra contain broad bands from

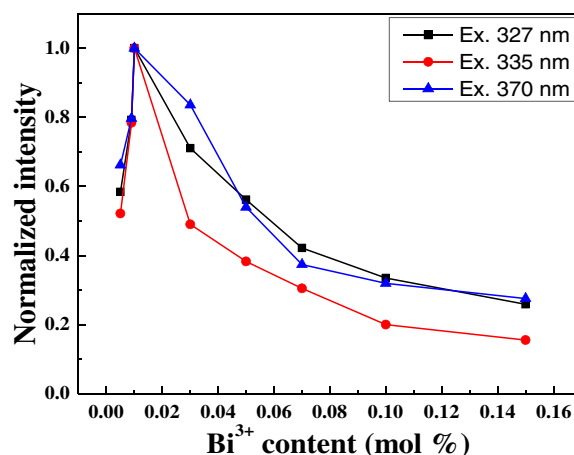


**Figure 5** Normalized intensity of as-synthesized  $\text{Sr}_3\text{Lu}_2(\text{BO}_3)_4:\text{xBi}^{3+}$  phosphor excited at 327 nm, 335 nm and 370 nm.

350 nm - 580 nm which are attributed to the emission properties of  $\text{Bi}^{3+}$  while the sharp lines ranging from 580 nm - 650 nm are due to the  $\text{Eu}^{3+}$  intra-configurational  $4f-4f$  located at transitions while the emission spectrum monitored at 410 nm contains two absorption peaks situated at which 334 nm and 371 nm. On the other hand, the excitation spectra monitored at 492 nm consist of two peaks located at 326 nm and 342 nm which is identical to the excitation spectra of  $\text{Sr}_3\text{Lu}_2(\text{BO}_3)_4:\text{Bi}^{3+}$ . The excitation spectra monitored at 610 nm contains broad excitation bands at around 300 nm - 400 nm which could be ascribed to the absorption of  $\text{Bi}^{3+}$ . The narrow peaks were due to the intra-configurational  $4f-4f$  transitions of  $\text{Eu}^{3+}$  located at 593 nm ( $^5\text{D}_0 \rightarrow ^7\text{F}_0$ ), 599 nm ( $^5\text{D}_0 \rightarrow ^7\text{F}_1$ ), 610 nm ( $^5\text{D}_0 \rightarrow ^7\text{F}_2$ ) and 631 nm ( $^5\text{D}_0 \rightarrow ^7\text{F}_3$ ). Spectral overlap between the emission band of the sensitizer and absorption band of the activator is essential to have an efficient energy transfer [13]. The spectral overlap of  $\text{Bi}^{3+}$  emission with the  $\text{Eu}^{3+}$  excitation spectra situated at 464 nm and 533 nm indicates successful energy transfer from  $\text{Bi}^{3+}$  to  $\text{Eu}^{3+}$ .

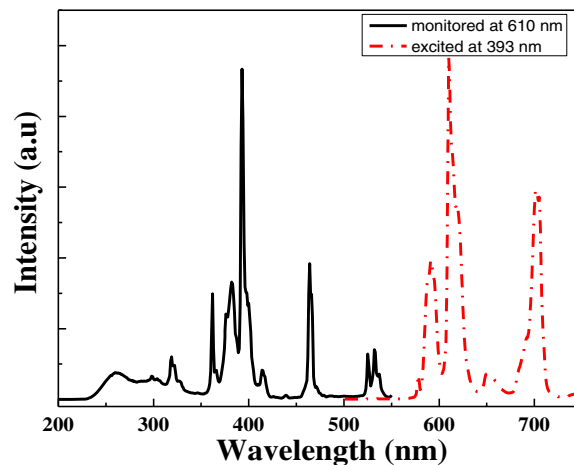
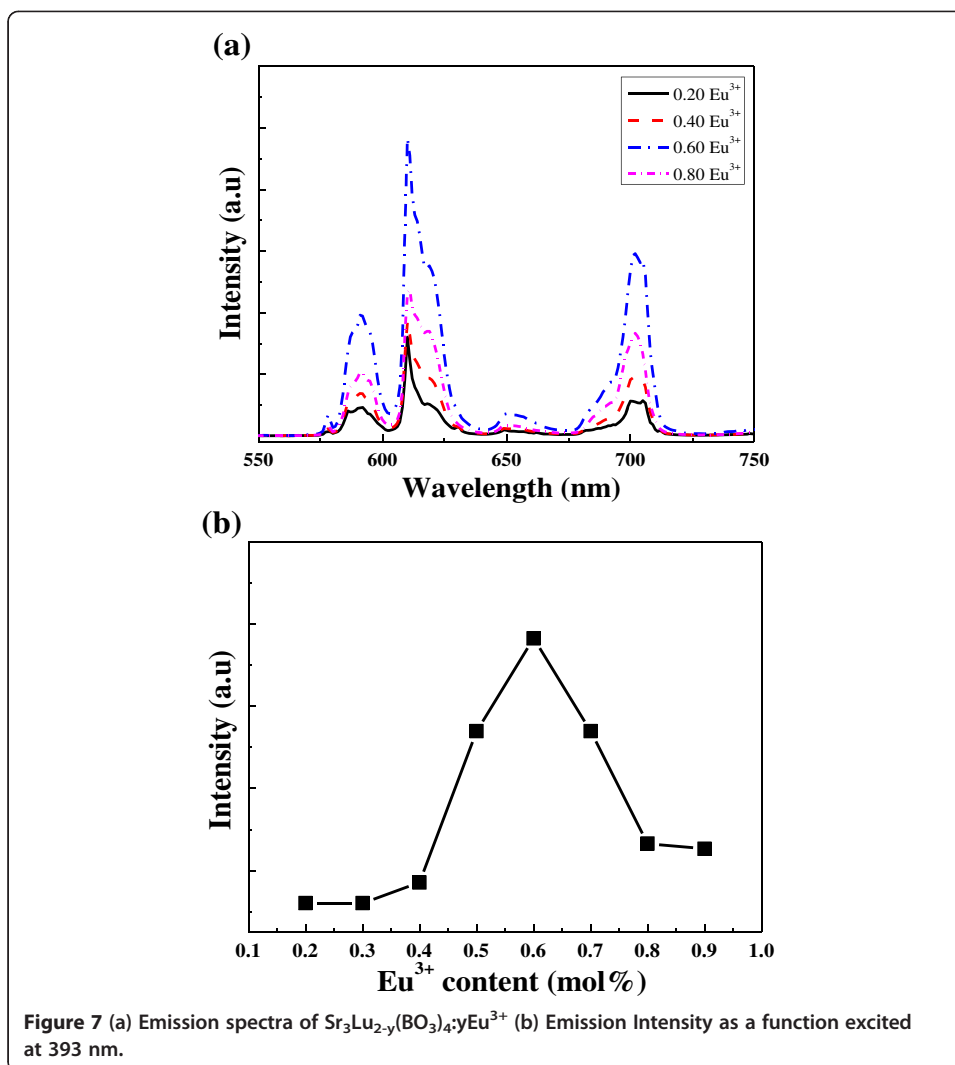


**Figure 6** PL and PLE spectra of as-synthesized  $\text{Sr}_3\text{Lu}_{1.20}(\text{BO}_3)_4:0.80\text{Eu}^{3+}$  phosphor.





Figures 9a and 9b exhibit the emission spectra of  $\text{Sr}_3\text{Lu}_{1.99-y}(\text{BO}_3)_4:0.01\text{Bi}^{3+}, y\text{Eu}^{3+}$  phosphors with varying concentrations of  $\text{Eu}^{3+}$  ( $y = 0.05, 0.10, 0.15, 0.20, 0.25, 0.35$ ) excited at 327 nm and 370 nm respectively. It was apparent that the energy absorbed by  $\text{Bi}^{3+}$  was transferred to  $\text{Eu}^{3+}$  and the emission of  $\text{Bi}^{3+}$  was quenched at higher  $\text{Eu}^{3+}$  concentration. Moreover, the figure indicates that the optimum concentration of  $\text{Bi}^{3+}$  co-activated  $\text{Eu}^{3+}$  was  $\text{Sr}_3\text{Lu}_{1.79}(\text{BO}_3)_4:0.01\text{Bi}^{3+}, 0.20\text{Eu}^{3+}$  and the intensity decreases eventually with a further increase in  $\text{Eu}^{3+}$  concentration.

Figure 10 further proves the energy transfer from  $\text{Bi}^{3+}$  to  $\text{Eu}^{3+}$ . It is evident that the intensity of  $\text{Bi}^{3+}$  decreases with the increase in  $\text{Eu}^{3+}$  concentration. This shows that the energy absorbed by  $\text{Bi}^{3+}$  is transferred to  $\text{Eu}^{3+}$ . Aside from spectral overlap, efficient energy transfer requires strong interactions it includes radiative transfer via photons which is almost distance independent and nonradiative transfer associated with the resonance between the acceptor and the donor that can be either an exchange interaction or multipolar interaction [15-19]. To calculate the critical transfer distance ( $R_c$ ) between the activators  $\text{Bi}^{3+}$  and  $\text{Eu}^{3+}$  the following equation is considered:



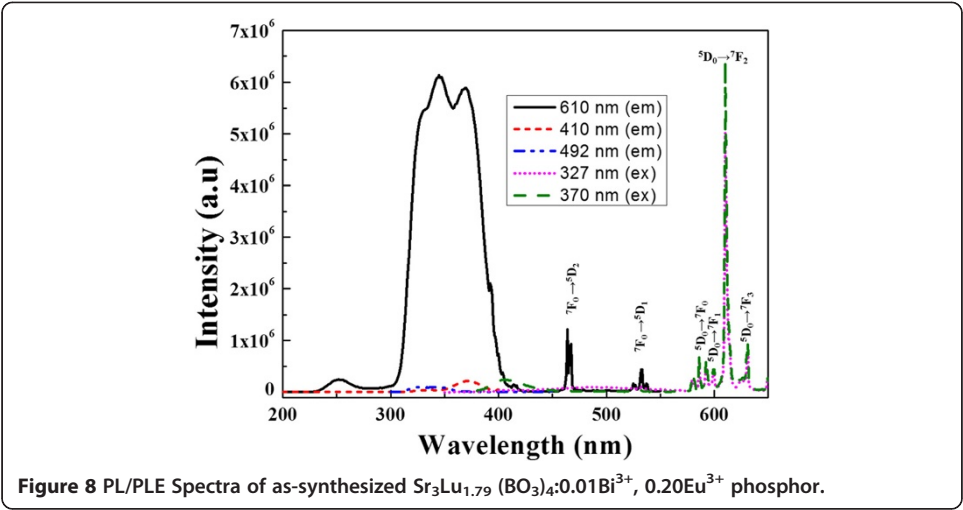


Figure 8 PL/PLE Spectra of as-synthesized  $\text{Sr}_3\text{Lu}_{1.79}(\text{BO}_3)_4:0.01\text{Bi}^{3+}, 0.20\text{Eu}^{3+}$  phosphor.

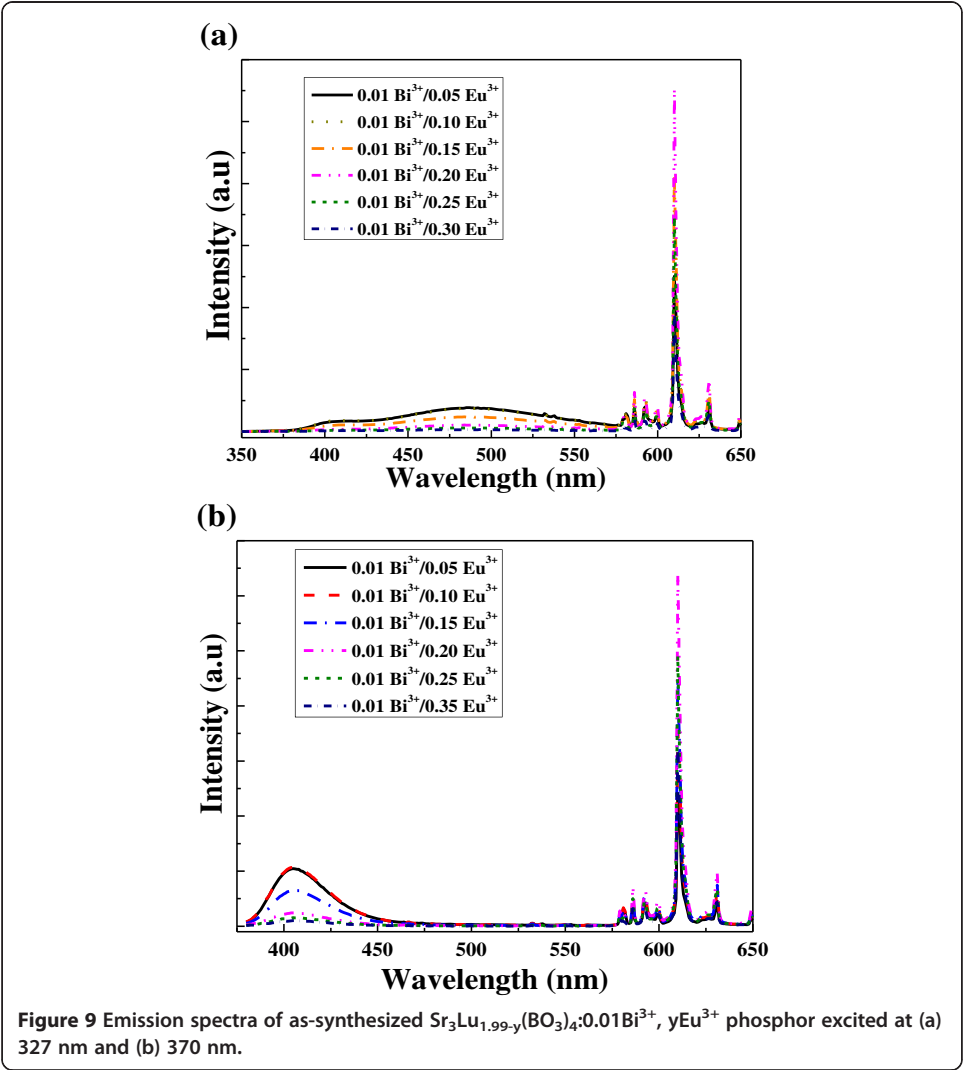


Figure 9 Emission spectra of as-synthesized  $\text{Sr}_3\text{Lu}_{1.99-y}(\text{BO}_3)_4:0.01\text{Bi}^{3+}, y\text{Eu}^{3+}$  phosphor excited at (a) 327 nm and (b) 370 nm.

$$R_c = 2 \left( \frac{3V}{4\pi X_c N} \right)^{1/3} \quad (1)$$

where  $V = 1077.54 \text{ \AA}^3$  is the volume of the unit cell,  $X_c = 0.21$  which is the total concentration of  $\text{Bi}^{3+}$  and  $\text{Eu}^{3+}$  at maximum luminescence intensity [16] and  $N = 8$  which represents the number of  $\text{Lu}^{3+}$  ions [20]. The critical distance of  $\text{Bi}^{3+}$  and  $\text{Eu}^{3+}$  was calculated to be  $10.70 \text{ \AA}$ . In an exchange interaction, the critical distance should be shorter than  $5 \text{ \AA}$  thus, it is rational to hypothesize that the mechanism involved is multipolar interaction [16-19]. According to Dexter's energy transfer expressions of multipolar interaction [16-19] and Reisfeld's transfer approximation [16,17] the following relation can be obtained:

$$\frac{\eta_o}{\eta} \propto C_{\text{Bi}+\text{Eu}}^{n/3} \quad (2)$$

where  $\eta_o$  and  $\eta$  are the luminescence quantum efficiency the sensitizer ( $\text{Bi}^{3+}$ ) in the absence and presence of the activator ( $\text{Eu}^{3+}$ ) respectively. The ratio of  $\eta_o/\eta$  can be estimated by the ratio of the relative luminescence intensities,  $I_{so}/I_s$  without and with the activator.  $C$  is the total concentration of  $\text{Bi}^{3+}$  and  $\text{Eu}^{3+}$  ions and  $n = 6, 8, 10$  which corresponds to dipole-dipole, dipole- quadrupole and quadrupole-quadrupole interaction [16-19]. The relationships between  $I_{so}/I_s$  and  $C_{\text{Bi}+\text{Eu}}$  excited at  $327 \text{ nm}$  is illustrated in Figure 11(a), (b) and (c). It is evident that graph for  $n = 6$  has the best-fitted linearity for both excitation. Therefore, the energy transfer from  $\text{Bi}^{3+}$  to  $\text{Eu}^{3+}$  was due to dipole-dipole interaction.

In order to further understand the energy transfer from  $\text{Bi}^{3+}$  to  $\text{Eu}^{3+}$  it is of high importance to discuss the energy transfer efficiency ( $\eta_T$ ) from the sensitizer to the activator depicted in Figure 12 and expressed by:

$$\eta_T = 1 - \frac{I_s}{I_{so}} \quad (3)$$

where  $I_s$  and  $I_{so}$  are the emission intensity of  $\text{Bi}^{3+}$  with and without  $\text{Eu}^{3+}$ , respectively. The  $\eta_T$  of  $\text{Sr}_3\text{Lu}_{1.99-y}(\text{BO}_3)_4:0.01\text{Bi}^{3+}, y\text{Eu}^{3+}$  was calculated as a function varying

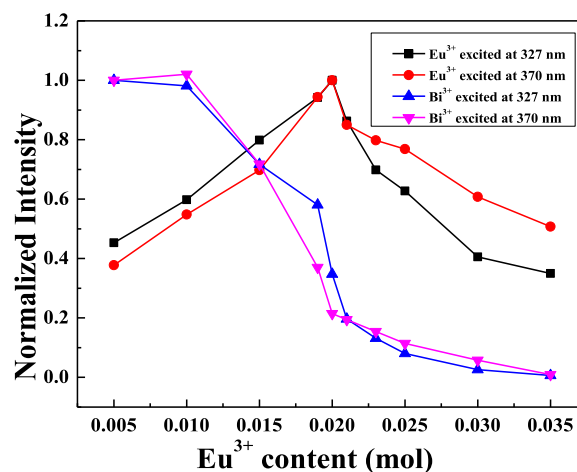
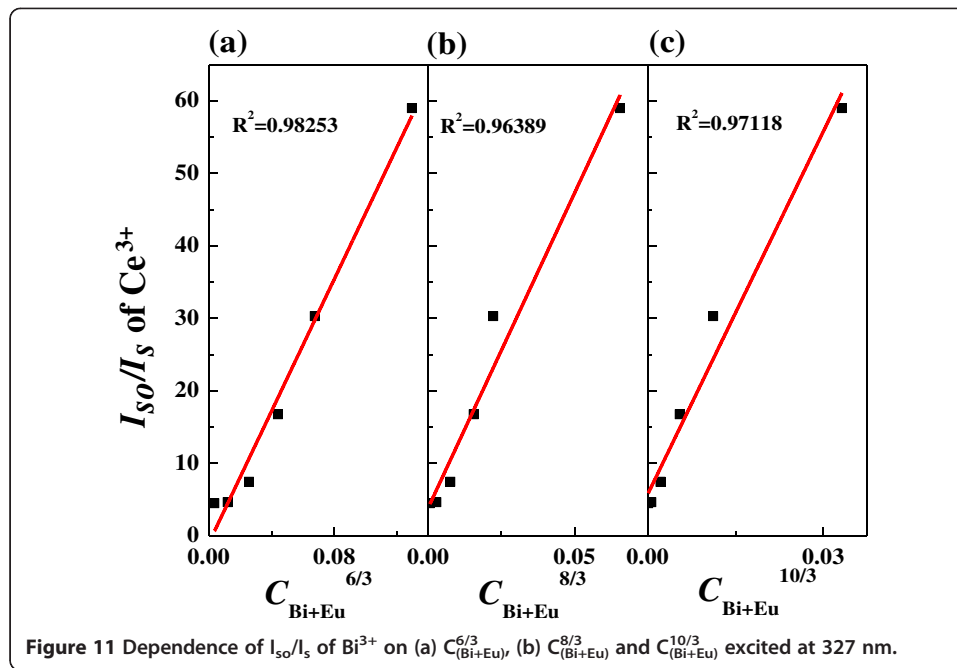
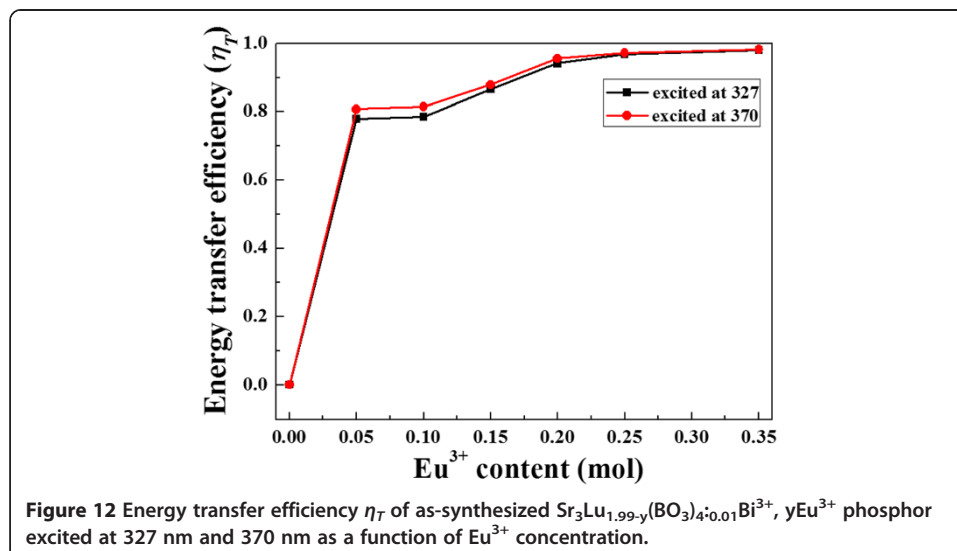


**Figure 10** Normalized PL intensity of as-synthesized  $\text{Sr}_3\text{Lu}_{1.99-y}(\text{BO}_3)_4:0.01\text{Bi}^{3+}, y\text{Eu}^{3+}$  phosphor.



concentration of  $\text{Eu}^{3+}$  which demonstrated that the energy transfer efficiency increases as the amount of activator  $\text{Eu}^{3+}$  increases.

With the intention of further investigating the energy transfer between  $\text{Bi}^{3+}$  and  $\text{Eu}^{3+}$ , the photoluminescence curve of  $\text{Bi}^{3+}$  in  $\text{Sr}_3\text{Lu}_{1.99-y}(\text{BO}_3)_4:0.01\text{Bi}^{3+}, y\text{Eu}^{3+}$  phosphors excited at 327 nm were measured and the corresponding lifetime ( $\tau$ ) of  $S_6$  and  $C_2$  site of  $\text{Bi}^{3+}$  were calculated as depicted in Figure 13. Since the decay curves are not exponential, therefore the samples were characterized using the average lifetime ( $\tau$ ) and were calculated using the following equation:



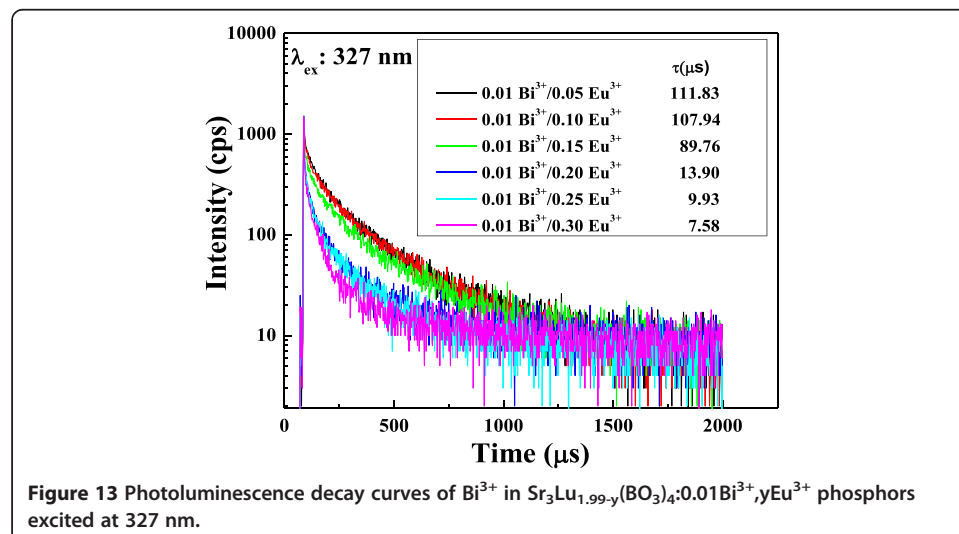
$$\tau = \frac{\int_0^{\infty} I(t)tdt}{\int_0^{\infty} I(t)dt} \quad (4)$$

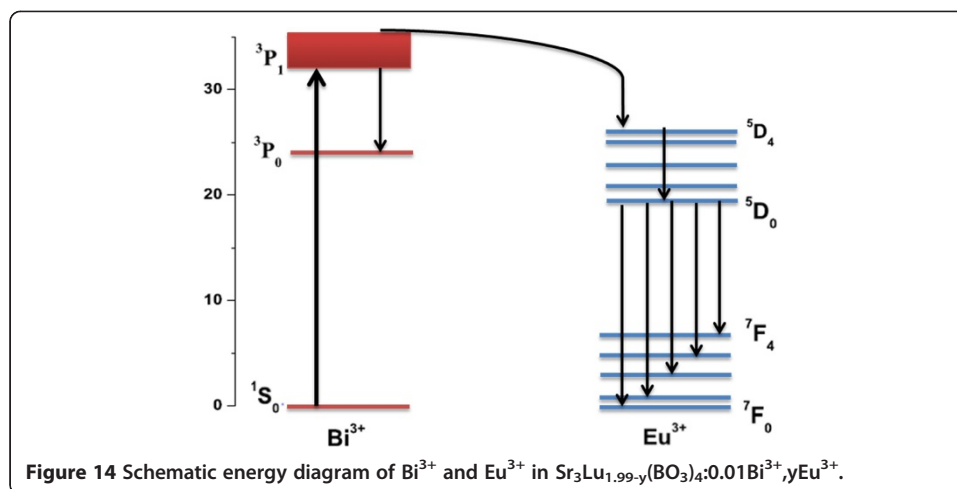
where  $I(t)$  is the intensity at time  $t$ . In the inset of Figure 13, the corresponding lifetime ( $\tau$ ) of each samples were given and calculated as 111.83  $\mu$ s, 107.94  $\mu$ s, 89.76  $\mu$ s, 13.90  $\mu$ s, 9.93  $\mu$ s and 7.58  $\mu$ s for  $\text{Sr}_3\text{Lu}_{1.99-y}(\text{BO}_3)_4:0.01\text{Bi}^{3+}, y\text{Eu}^{3+}$  ( $y = 0.05, 0.10, 0.15, 0.20, 0.25, 0.30$ ) respectively and it is evident that as the doping concentration of  $\text{Eu}^{3+}$  increases, the  $\tau$  of  $\text{Bi}^{3+}$  decreases which confirms the energy is successfully transferred from the sensitizer to the activator [9,16].

The schematic energy transfer diagram between  $\text{Bi}^{3+}$  and  $\text{Eu}^{3+}$  is presented in Figure 14. Upon excitation at 327 nm, 335 nm and 370 nm the  $\text{Bi}^{3+}$  are stimulated from the ground state  $^1\text{S}_0$  to excited state  $^3\text{P}_1$ . In Figure 3, it was presented that there are two sites in level  $^3\text{P}_1$ ,  $\text{S}_6$  and  $\text{C}_2$  site which are responsible for the blue and green emission of  $\text{Bi}^{3+}$  [20]. Subsequently, the absorbed energy can be transferred to the  $^5\text{D}_4$  and level of  $\text{Eu}^{3+}$  and the emission of  $\text{Bi}^{3+}$  is quenched as the concentration of  $\text{Eu}^{3+}$  increases. The excited state of  $\text{Eu}^{3+}$  at  $^5\text{D}_4$  relaxes non-radiatively to the lowest component of  $^5\text{D}$  accompanied by broad emission bands as shown in Figure 9a-b and successively returns to its ground state  $^7\text{F}_0$ .

#### CIE coordinates

The chromaticity coordinates of the phosphor  $\text{Sr}_3\text{Lu}_{1.99-y}(\text{BO}_3)_4:0.01\text{Bi}^{3+}, y\text{Eu}^{3+}$  and its corresponding relative intensity are calculated and presented in Table 1 and Figure 15, respectively. It depicts that the co-activation of  $\text{Bi}^{3+}$  and  $\text{Eu}^{3+}$  has increased the  $^5\text{D}_0 \rightarrow ^7\text{F}_2$  attributed to  $\text{Eu}^{3+}$  which was responsible for its red emission. At 327 nm excitation, the relative intensity of  $\text{Sr}_3\text{Lu}_{1.79}(\text{BO}_3)_4:0.01\text{Bi}^{3+}, 0.20\text{Eu}^{3+}$  was enhanced by 201% although, its CIE coordinates indicates that it has an orange hue. On the other hand, when excited at 370 nm, the intensity was improved by 265% and according to its CIE coordinates, it has a bright red hue. Figure 16 shows the PL spectra of composition-optimized SLBO:Bi,





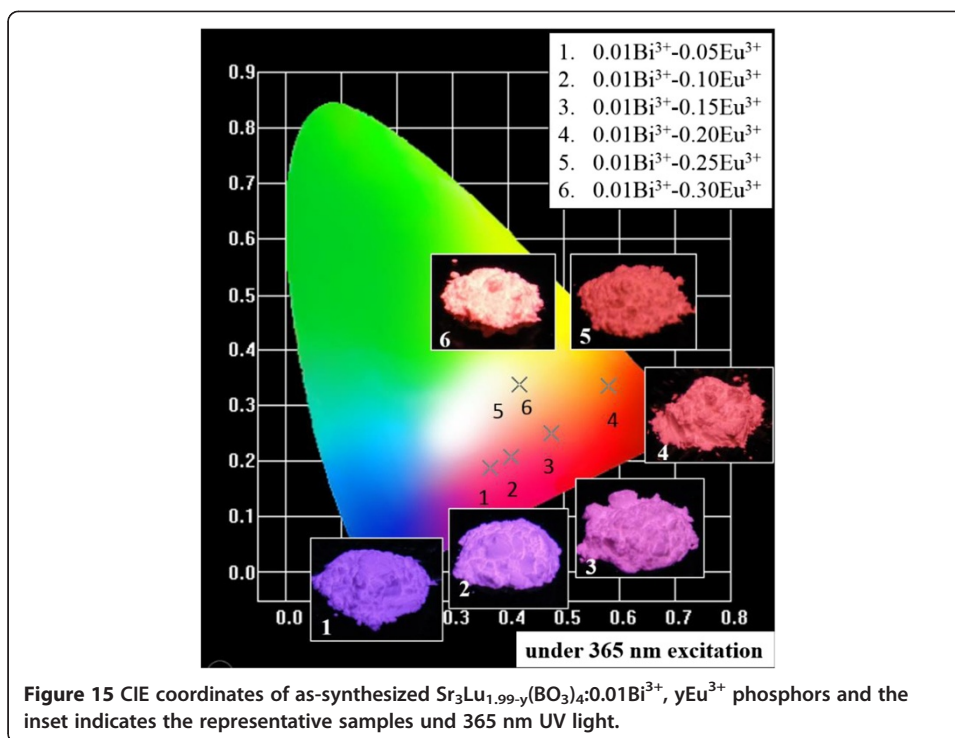
Eu phosphor and commercial red-emitting phosphor –  $\text{Y}_2\text{O}_3:\text{Eu}^{3+}$  (KX-681, Kasei co.) under excitation of 393 nm. The inset in Figure 16 displays the phosphor images of these two phosphors excited at 365 nm in UV box. The PL intensity of SLBO is about 32% of commercial phosphor. The measurement of quantum efficiency (QE) for SLBO and  $\text{Y}_2\text{O}_3:\text{Eu}^{3+}$  are carried out under excitation of 393 nm in the integrating sphere. The QE of SLBO and  $\text{Y}_2\text{O}_3:\text{Eu}^{3+}$  were determined to be 28% and 91%, respectively. It is believed that the QE could be further improved by tuning synthetic parameters, such as starting materials, synthetic approach and fluxes. The inset in Figure 16 also demonstrates that as-synthesized SLBO:Bi,Eu phosphor gives a bright and intense red hue.

## Conclusions

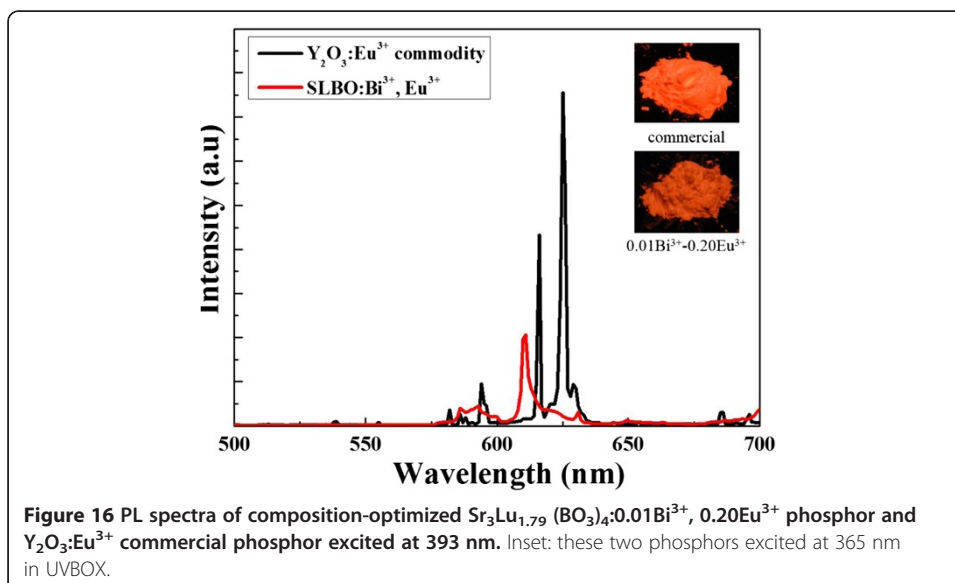
$\text{Sr}_3\text{Lu}_2(\text{BO}_3)_4:\text{Bi}^{3+}$ ,  $\text{Eu}^{3+}$  were effectively synthesized by a solid state reaction and pure phase phosphors were successfully synthesized. Changing the excitation wavelengths from 320 ~ 370 nm greatly affects the emission spectra of  $\text{Sr}_3\text{Lu}_2(\text{BO}_3)_4:\text{Bi}^{3+}$ . Hence,

**Table 1** CIE coordinates and relative intensity of  $\text{SLBO}:\text{Bi}^{3+},\text{Eu}^{3+}$  phosphors

Phosphors	Excitation Wavelength (nm)	CIE chromaticity coordinates		$^5\text{D}_0 \rightarrow ^7\text{F}_2$ relative intensity
		x	y	
$\text{Sr}_3\text{Lu}_{1.94}(\text{BO}_3)_4:0.01\text{Bi}^{3+},0.05\text{Eu}^{3+}$	327	0.3087	0.3182	1.00
$\text{Sr}_3\text{Lu}_{1.89}(\text{BO}_3)_4:0.01\text{Bi}^{3+},0.10\text{Eu}^{3+}$	327	0.3386	0.3199	1.32
$\text{Sr}_3\text{Lu}_{1.84}(\text{BO}_3)_4:0.01\text{Bi}^{3+},0.15\text{Eu}^{3+}$	327	0.4029	0.3266	1.65
$\text{Sr}_3\text{Lu}_{1.79}(\text{BO}_3)_4:0.01\text{Bi}^{3+},0.20\text{Eu}^{3+}$	327	0.5191	0.3395	2.01
$\text{Sr}_3\text{Lu}_{1.74}(\text{BO}_3)_4:0.01\text{Bi}^{3+},0.25\text{Eu}^{3+}$	327	0.5303	0.3393	1.38
$\text{Sr}_3\text{Lu}_{1.64}(\text{BO}_3)_4:0.01\text{Bi}^{3+},0.35\text{Eu}^{3+}$	327	0.5365	0.3386	1.11
$\text{Sr}_3\text{Lu}_{1.94}(\text{BO}_3)_4:0.01\text{Bi}^{3+},0.05\text{Eu}^{3+}$	370	0.3678	0.1870	1.00
$\text{Sr}_3\text{Lu}_{1.89}(\text{BO}_3)_4:0.01\text{Bi}^{3+},0.10\text{Eu}^{3+}$	370	0.4039	0.2065	1.45
$\text{Sr}_3\text{Lu}_{1.84}(\text{BO}_3)_4:0.01\text{Bi}^{3+},0.15\text{Eu}^{3+}$	370	0.4772	0.2512	1.85
$\text{Sr}_3\text{Lu}_{1.79}(\text{BO}_3)_4:0.01\text{Bi}^{3+},0.20\text{Eu}^{3+}$	370	0.5800	0.3356	2.65
$\text{Sr}_3\text{Lu}_{1.74}(\text{BO}_3)_4:0.01\text{Bi}^{3+},0.25\text{Eu}^{3+}$	370	0.4186	0.3377	2.03
$\text{Sr}_3\text{Lu}_{1.64}(\text{BO}_3)_4:0.01\text{Bi}^{3+},0.35\text{Eu}^{3+}$	370	0.4201	0.3377	1.34



the energy distribution of blue and green emission is highly dependent on the excitation wavelengths. The concentration quenching for  $\text{Sr}_3\text{Lu}_{2-x}(\text{BO}_3)_4:x\text{Bi}^{3+}$ ,  $\text{Sr}_3\text{Lu}_{2-y}(\text{BO}_3)_4:y\text{Eu}^{3+}$  and  $\text{Sr}_3\text{Lu}_{2-x-y}(\text{BO}_3)_4:x\text{Bi}^{3+}, y\text{Eu}^{3+}$  are 1 mol%, 60 mol% and 20 mol%, respectively. The spectral overlap of the emission spectra of  $\text{Bi}^{3+}$  and the excitation band of  $\text{Eu}^{3+}$  depicts an efficient energy transfer from  $\text{Bi}^{3+}$  to  $\text{Bi}^{3+}$ . Moreover, it was shown that the emission intensity of  $\text{Bi}^{3+}$  quenches as the concentration of  $\text{Eu}^{3+}$  increases hence, the energy absorbed by  $\text{Bi}^{3+}$  was transferred to  $\text{Eu}^{3+}$ . The critical distance of  $\text{Eu}^{3+}$  was determined to be 10.7 Å. The relative intensity of  $\text{Sr}_3\text{Lu}_{1.79}(\text{BO}_3)_4:0.01\text{Bi}^{3+}, 0.20\text{Eu}^{3+}$  at 327 nm and 370 nm



were dramatically enhanced by 201% and 265%, respectively. The results indicate that  $\text{Sr}_3\text{Lu}_2(\text{BO}_3)_4:\text{Bi}^{3+}$ ,  $\text{Eu}^{3+}$  is a potential novel red-emitting UV LED phosphor for display application.

#### Competing interests

The authors declare that they have no competing interests.

#### Authors' contributions

IVBM performed the experiment, analyzed the data and wrote the paper. PCL refined the graphs, tables and other essential information about this paper. WRL guided and scrutinized all the experiments and edited the paper. All the authors discussed and analyzed the results and commented on the manuscript. All authors read and approved the final manuscript.

#### Authors' information

IVBM and PCL are both taking their Master's Degree in Chung Yuan Christian University, ROC Taiwan. WRL has a Ph.D. degree and is currently an assistant professor in Chung Yuan Christian University and is affiliated with Industrial Technology Research Institute of Taiwan (ITRI), ROC Taiwan.

#### Acknowledgment

The work is financially supported from NSC under contracts no. of 102-2221-E-033-050-MY2 and 102-3011-P-033-003.

Received: 1 March 2014 Accepted: 1 July 2014

Published: 16 July 2014

#### References

- Liu WR, Lin CC, Chiu YC, Yeh YT, Jang SM, Liu RS:  $\text{ZnB}_2\text{O}_4:\text{Bi}^{3+}$ ,  $\text{Eu}^{3+}$ : a highly efficient, red emitting phosphor. *Opt Express* 2010, **18**:2946–2951.
- Rui Z, Xiang W: Preparation and luminescent characteristics of  $\text{Sr}_3\text{RE}_2(\text{BO}_3)_4:\text{Dy}^{3+}$  (RE = Y, La, Gd). *J Alloys Compd* 2011, **509**:1197–1200.
- Guo C, Ding X, Seo HJ, Ren Z, Bai J: Double emitting phosphor  $\text{NaSr}_4(\text{BO}_3)_3:\text{Ce}^{3+}$ ,  $\text{Tb}^{3+}$  for near UV light-emitting diodes. *Opt Laser Tech* 2011, **43**:1351–1354.
- Zhou H, Yu X, Qian S, Shi R, Wang T, Yang P, Yang Y, Qui J: Photoluminescence properties of  $\text{Eu}^{3+}$  and  $\text{Bi}^{3+}$  co-doped  $\text{Ca}_3\text{SnSi}_2\text{O}_9$  phosphors through energy transfer. *MRS* 2013, **48**:2396–2398.
- Liu WR, Yeh CW, Huang CH, Lin CC, Chiu YC, Yeh YT, Liu RS: (Ba, Sr)  $\text{Y}_2\text{Si}_2\text{Al}_2\text{O}_7:\text{Eu}^{2+}$ : a novel near-ultraviolet converting green phosphor for white-light emitting diodes. *J Mat Chem* 2011, **21**:3740–3744.
- Zhang ZW, Sun XY, Liu L, Peng YS, Shen XH, Zhang WG, Wang DJ: Synthesis and luminescence properties of novel  $\text{LiSr}_4(\text{BO}_3)_3:\text{Dy}^{3+}$  phosphors. *Ceram Int* 2013, **39**:1723–1729.
- Wan L, Lu S, Sun L, Qu X:  $\text{Bi}^{3+}$  enhanced red emission in  $\text{Sr}_{0.5}\text{Ca}_{0.4}\text{MoO}_4:\text{Eu}^{3+}$  phosphor. *Opt Mat* 2014, **36**:628–632.
- Wang Z, Liang H, Gong M, Su Q: Novel red phosphor  $\text{Bi}^{3+}$ ,  $\text{Sm}^{3+}$  co-activated  $\text{NaEu}(\text{MoO}_4)_2$ . *Opt Mat* 2007, **29**:896–900.
- Zhu H, Xia Z, Liu H, Mi R, Hui Z: Luminescence properties and energy transfer of  $\text{Bi}^{3+}/\text{Eu}^{3+}$ -codoped  $\text{Ca}_{10}(\text{PO}_4)_6\text{F}_2$  phosphors. *MRS* 2013, **48**:3513–3517.
- Ju G, Hu Y, Wu H, Yang Z, Fu C, Mu Z, Kang F: A red-emitting heavy doped phosphor  $\text{Li}_6\text{Y}(\text{BO}_3)_3:\text{Eu}^{3+}$  for white light-emitting diodes. *Opt Mat* 2011, **33**:1297–1301.
- Liu WR, Chui YC, Tung CY, Yeh YT, Jang SM, Chen TM: A study on the luminescence properties of  $\text{CaAlBO}_4:\text{RE}^{3+}$  (RE = Ce, Tb and Eu). *J Electrochem Soc* 2008, **155**:J252–J255.
- Park WJ, Jung MK, Yoon DH: Influence of  $\text{Eu}^{3+}$ ,  $\text{Bi}^{3+}$  co-doping content on photoluminescence of  $\text{YVO}_4$  red phosphors induced by ultraviolet excitation. *Sensors Actuators B* 2007, **126**:324–327.
- Huang J, Chen Y, Gong X, Lin Y, Luo Z, Huang Y: Spectral and laser properties of  $\text{Er}:\text{Yb}:\text{Sr}_3\text{Lu}_2(\text{BO}_3)_4$  crystal at 1.5–1.6  $\mu\text{m}$ . *Opt Soc* 2013, **3**:1885–1892.
- He L, Wang Y: Synthesis of  $\text{Sr}_3\text{Y}_2(\text{BO}_3)_4:\text{Eu}^{3+}$  and its photoluminescence under UV and VUV excitation. *J Alloys Compd* 2007, **431**:226–229.
- Ju G, Hu Y, Chen L, Wang X, Mu Z, Wu H, Kang F: White-light generation and energy transfer in  $\text{Y}_2\text{O}_3:\text{Bi}$ ,  $\text{Eu}$  phosphor for ultraviolet light-emitting diodes. *J Electrochem Soc* 2011, **10**:J294–J299.
- Xia Z, Liu RS: Tunable Blue-Green Color Emission and Energy Transfer of  $\text{Ca}_2\text{Al}_3\text{O}_6\text{F}:\text{Ce}^{3+}$ ,  $\text{Tb}^{3+}$  Phosphors for Near-UV White LEDs. *J Phys Chem* 2012, **116**:15604–15609.
- Jin Y, Hu Y, Chen L, Wang X, Mu Z, Ju G, Yang Z: A novel emitting color tunable phosphor  $\text{Ba}_3\text{Gd}(\text{PO}_4)_3:\text{Ce}^{3+}$ ,  $\text{Tb}^{3+}$  based on energy transfer. *Phys B* 2014, **436**:105–110.
- Fu X, Fang L, Niu S, Zhang H: Luminescence properties and energy transfer investigations of  $\text{SrMgSi}_2\text{O}_6:\text{Ce}$ ,  $\text{Tb}$  phosphors. *J Lumin* 2013, **142**:163–166.
- Sun J, Sun Y, Lai J, Xia Z, Du H: Luminescence properties and energy transfer investigations of  $\text{BaAl}_2\text{B}_2\text{O}_7:\text{Ce}^{3+}$ ,  $\text{Tb}^{3+}$  phosphors. *J Lumin* 2012, **132**:3048–3052.
- Kuo TW, Chen TM: Synthesis and luminescence properties of  $\text{Eu}^{3+}$ ,  $\text{Ce}^{3+}$  and  $\text{Tb}^{3+}$ -activated  $\text{Sr}_3\text{La}_2(\text{BO}_3)_4$  under UV excitation. *J Lumin* 2010, **130**:483–487.

doi:10.1186/s40539-014-0013-6

**Cite this article as:** Maggay et al.: Enhanced luminescence intensity of novel red-emitting phosphor  $-\text{Sr}_3\text{Lu}_2(\text{BO}_3)_4:\text{Bi}^{3+},\text{Eu}^{3+}$  via energy transfer. *Journal of Solid State Lighting* 2014 **1**:13.